MRS Advances © 2016 Materials Research Society
DOI: 10.1557/adv.2016.368

Effect of Ammonium Acetate Concentration on the Structural and Optical Properties of CdS Thin Film Grown by Chemical Bath Deposition Technique

Hamda A. Al-Thani[1], Abeer A. Al Yafeai[1], and Falah S. Hasoon[1]
[1]National Energy and Water Research Center (NEWRC), POBOX 54111, Abu Dhabi, UAE

ABSTRACT

This study focuses on understanding the influence of incorporating Ammonium Acetate into the chemical bath used for the deposition of CdS thin films, on its optical, morphology, and microstructural properties. Thus, CdS thin films were deposited on 1" × 2" microscopic glass substrates using chemical bath deposition (CBD) technique. The deposition process was carried out in a double jacket beaker with fixed chemical bath temperature of 90°C for a deposition time of 40 min. The chemical bath solution consisted of fixed concentrations of Cadmium Acetate, Thiourea, and Ammonium Hydroxide; with corresponding values of 4.8×10^{-4}M; 0.97×10^{-4}M; and 0.2M, respectively. However, Ammonium Acetate was incorporated into the deposition bath with concentrations that were varied from 3.0 mM to 12.2 mM. Meanwhile, for comparison purposes associated to the initial physical and chemical properties of the CdS films; reference CdS films were deposited under the same above chemical bath conditions, but in the absence of Ammonium Acetate. The pH of the chemical bath was measured during the deposition process. The films' morphology and the chemical composition were examined by Field Emission Scanning Electron Microscopy (FE-SEM), and the Energy Dispersive spectrometer (EDS), respectively. The X-Ray Diffraction (XRD) $\theta/2\theta$ technique was applied to study the structure of the films, including the lattice parameters. Atomic Force Microscopy (AFM) was used to examine the films topography and to determine the root-mean-square (RMS) surface roughness of the films as well as the grain size. Dektak Surface Profilometer was used to determine the CdS films' thickness, where the films' optical properties were measured using UV-Vis-NIR spectrometer. Optical energy band gap (Eg), and absorption coefficient (α) were calculated from the transmission spectral data.

INTRODUCTION

Cadmium Sulfide (CdS) thin films play an important role in the development of cost effective and reliable photovoltaic devices. CdS thin films have been used as a junction partners in CdTe and CIGS based solar cells for many years. In addition to its suitable direct band gap, high absorption coefficient and low resistivity [1-4]; CdS buffer layer provides full coverage of an epitaxial layer for the rough polycrystalline surface of the absorber layer. This results in improving the device photocurrent by enhancing the solar cell absorption spectra in the UV range and in the cell circuit voltage [5,6].

There are several techniques that are used for CdS thin film deposition as such chemical bath deposition (CBD) [7,8], vacuum evaporation [9], sputtering [10], electrodeposition [11], molecular beam epitaxy (MBE) [12,13], screen printing [14], metal organic chemical vapor deposition (MOCVD) [15,16], pulsed laser ablation [17], close-space sublimation (CSS) [18], and Spray pyrolysis [19]. However, out of the previously mentioned techniques, the chemical bath deposition (CBD) is considered is the most common technique applied to achieve the best

device performance so far. Where the highest efficiency currently reported for both CIGS and CdTe based solar cells are 21.7% and 21.5%, respectively [20]. The chemical bath deposition of CdS thin films (CBD-CdS) is considered as low cost technique, and easy to upscale and confine the waste products [21-23]. The deposition technique of CdS thin films is based on the reaction between Cd and S ions in an alkaline solution. The slow release of Cd ions is achieved by adding a complexing agent to the Cd salt to form cadmium complex species, while S ions are supplied by thiourea hydrolysis. During the deposition two reactions occur simultaneously and competing with each other. The first one is heterogeneous reaction (also known as ion-by-ion growth) which is the preferred reaction that results in forming an adherent and dense film to the substrate. Whereas, the other reaction is homogenous (also known as cluster-by-cluster growth) which results in forming a porous layer consists of precipitates of the CdS colloids in the bulk of the solution [24-26]. Depends on the deposition conditions, a thick film with a duplex structure might be formed that consists of an inner adherent dense layer and an over layer that is porous and less adherent. Saturation in film thickness also was reported for CdS thin films grown by CBD [25-27].

The quality and stoichiometry of the films depends on the deposition conditions such as stirring condition, PH of the solution [28,29], deposition time and temperature [3,8], as well as the relative concentration of the reactants [25,30-32]. For example it has been reported that the grain size of CdS films increases with increasing the ammonia concentration [31]. Also, the high concentration of ammonia results in second phase formation that affects the crystallinity of CdS film. The Ratio of Cadmium Acetate to the ammonium acetate was found to have a significant effect to increase the relative thickness yield of CdS films per cycle in multiple and continuous dip deposition process relative to that obtained in single dip deposition process [33, 34]. This paper focuses on understanding the impact of varying the concentration of ammonium acetate in the chemical bath deposition of CdS films, on its microstructural and optical properties as well as its stoichiometry.

EXPERIMENTAL

CdS thin films were deposited on 1"×2" microscopic glass substrates using chemical bath deposition (CBD) technique. The deposition process was carried out in a 600 ml double jacket beaker with fixed chemical bath temperature of 90 °C for a deposition time of 40 min. The chemical bath solution consisted of fixed concentrations of Cadmium Acetate as a source of Cd^{++} ions, Thiourea as a source of S^{-} ions, and Ammonium Hydroxide as a complexing agent; with concentrations of 4.8×10^{-4} M; 0.97×10^{-4} M; and 0.2 M, respectively. Ammonium Acetate was incorporated into the deposition bath with concentrations that were varied from 3.0 mM to 12.2 mM. Meanwhile, for comparison purposes associated to the initial physical and chemical properties of the CdS films; reference CdS films were deposited under the same above chemical bath conditions, but in the absence of Ammonium Acetate.

Prior to the deposition the double jacket beaker was placed on a magnet stirrer, filled with the high purity DI, and then connected to the constant temperature bath to heat the DI water up to the setting temperature of 90 °C. The volume of the high purity DI in the jacket beaker was varied according to each performed deposition process from 554.7 ml to 548 ml. This is to maintain the concentrations of the above chemicals used in this process controlled as required. Also, the magnetic stirrer was used to promote ion-by-ion heterogeneous growth on the substrate. The microscopic glass substrates were ultrasonically rinsed several times using high

purity DI water. The substrates and its holder were loaded in the water jacket beaker while the water was heating. The Cadmium Acetate, Ammonium Acetate, and Ammonium Hydroxide were added when the water temperature got stabilized at 85 °C. Note that the concentration of Ammonium Acetate was varied from one deposition process to another, with a range from 3.0 mM to 12.2 mM. However for the reference film deposition process; the Ammonium Acetate incorporation into the bath was eliminated. The deposition process is considered initiated by the addition of Thiourea using titration, when the bath reached stable temperature of 90 °C. The complete deposition process was performed for a total period of 40 min out of which the first 15 min was spent for Thiourea titration. The pH of the bath was measured at the last 2 min before the completion of each deposition process. Eventually after the deposition process was completed, the substrates were removed from the deposition bath and they were rinsed in high purity DI water. Then they were ultrasonically rinsed several times in DI water to help remove particulates from the film surface. Final rinse was performed for the films in high purity DI water, then the films were blown dry with nitrogen.

Subsequently, the films' morphology and the chemical composition were examined by Field Emission Scanning Electron Microscopy (FE-SEM), and the Energy Dispersive spectrometer (EDS), respectively. The X-Ray Diffraction (XRD) $\theta/2\theta$ technique was applied to study the structure of the films, including the lattice parameters. Atomic Force Microscopy (AFM) was used to examine the films topography and to determine the root-mean-square (RMS) surface roughness of the films and the grain size. Dektak Surface Profilometer was used to determine the CdS films' thickness, whereas the films' optical properties were measured using UV-Vis-NIR spectrometer. Optical energy band gap (Eg), and absorption coefficient (α) were calculated from the transmission spectral data.

RESULTS AND DISCUSSION

Figure 1 shows the measured pH values of the chemical bath during the deposition of the CdS films as a function of the investigated range of Ammonium Acetate concentrations. It can be noticed that the pH value decreases with increasing the Ammonium Acetate concentration, which can be correlated to the formation of Cadmium Cyanamide that is weakly soluble compound and to the increase consumption of the Hydroxide ions in the chemical bath [25].

Prior incorporating Ammonium Acetate, the deposition bath has a pH value of 9.2 that decreases and reaches its minimum of 8.2 with increasing the Ammonium Acetate concentration from 3.0 mM up to 12.2 mM. In spite of only varying the concentration of Ammonium Acetate and maintaining the other parameters of the chemical bath deposition fixed; as such the concentrations of Cadmium Acetate, Thiourea, and Ammonium Hydroxide in addition to the deposition bath temperature and time. Hence the growth rate of the chemical bath deposited CdS (CBD-CdS) thin films is linearly increasing with Ammonium Acetate concentration then it reaches a plateau with further increasing the Ammonium Acetate concentration of the deposition bath. This is as indicated from the CdS films thickness measurements, shown in figure 2. Consequently, the CdS films thickness increases from 68 Å, for the reference CdS film, to 593 Å upon incorporating Ammonium Acetate into the deposition bath with concentrations that vary from 3.0 mM up to intermediate value of 4.89 mM. Whereas, with further increasing the Ammonium Acetate concentration, CBD-CdS films thickness tends to form a plateau with an average thickness of 1035 Å.

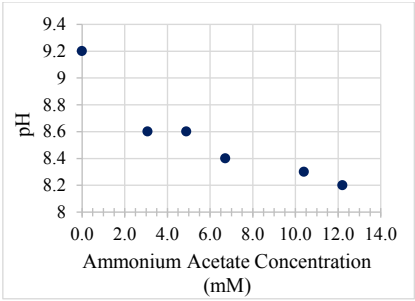

Figure 1. PH of the CdS deposition bath as a function of Ammonium Acetate concentration.

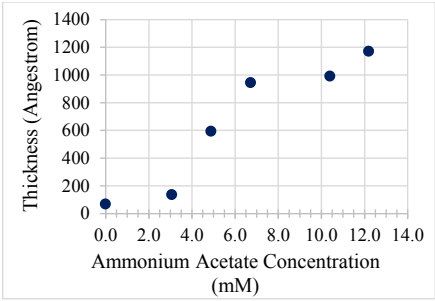

Figure 2. Thickness of the deposited CdS films as a function of Ammonium Acetate concentration of the chemical bath.

At low concentrations of Ammonium Acetate and relatively higher pH of the bath, the growth of the CdS films can be due to major contribution of heterogeneous reaction as a result a compact and adherent inner-layer of specular film is formed. On the other hand, at high investigated range of Ammonium Acetate concentrations and relatively lower pH of the bath; the appeared plateau in the growth rate, by means of the observed saturation of the film thickness can be due to the formation of a secondary layer of porous CdS and other Cd-compounds precipitates on top of dense CdS inner layer. This secondary layer is formed as a result of significant contribution of homogenous reaction, which is promoted by low rate of thiourea hydrolysis that is reduced with decreasing the pH of the deposition bath and by increasing the hydroxo-complexes and cadmium amine complexes species in the deposition bath [25, 35,36].

The chemical compositions of the CdS films were determined using EDS at electron probe accelerating voltage of 15 KeV. The EDS spectrums revealed presence of Cd and S in all films, and other elements such as O, Na, Mg, Al, Si, and Ca that are originated from the glass substrates. Furthermore, as illustrated in figure 3, the EDS results showed deviation from compositional stoichiometry at high Ammonium Acetate concentrations; where the Cd:S ratio increases slightly beyond 1. This deviation from stoichiometry starts to increase at Ammonium Acetate concentration of 6.7 mM until it eventually gets stabilized at higher concentrations with average Cd:S ratio of 1.29. It seems that the release of sulfide ions and its incorporation is affected by the concentration of Ammonium Acetate, lower pH bath and slower rate of thiourea hydrolysis. Therefore, the released sulfide ions become not efficient enough to correspond to a stoichiometric pure CdS film. At this level of Ammonium Acetate concentration, oxygen impurities such as $Cd(OH)_2$ and/or cyanamide impurities such as $CdCN_2$ can be formed and get incorporated into the CBD-CdS films [36-38]. However, investigation about possible existence of impurities in the CBD-CdS films and its correlation with the Ammonium Acetate concentration in the deposition bath, is beyond the scope of this research work and it is a subject for further investigation.

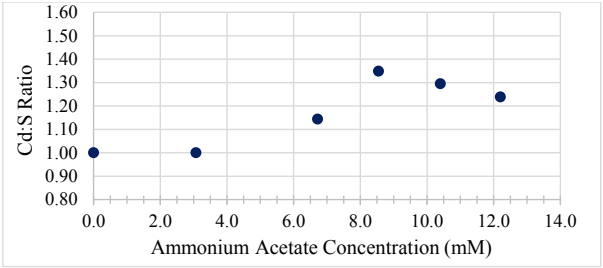

Figure 3. Cd:S ratio for CBD-CdS films as a function of corresponding Ammonium Acetate concentration of the deposition bath.

The morphology of the films is illustrated by the SEM images shown in figures 4(a) and (b) for CBD-CdS films with associated Ammonium Acetate concentrations of 3 mM and 10 mM, respectively. The SEM images show that all CdS films are characterized by tapered crystallites with domed tops. Concern the continuity of the reference CdS film, the film revealed large discontinuity in the film coverage and free of pinholes. However, upon incorporating Ammonium Acetate into the deposition bath with low concentrations, the corresponding deposited CdS films exhibit continuous film coverage, with small grain size. The grains of the deposited CdS films become larger in size as the concentration of Ammonium Acetate increases in the deposition bath.

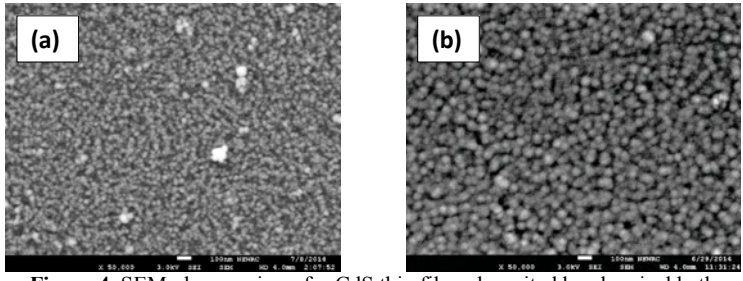

Figure 4. SEM planner views for CdS thin films deposited by chemical bath, where Ammonium Acetate concentration is (a) 3 mM, and (b) 10 mM.

Figure 5(a-e) and figure 6 illustrate respectively the AFM topography images for the CdS films and its associated grain diameter analysis as performed using AFM Nano-Scope Analysis software. The topography of the reference CdS film exhibits mono-modal and self-similar distribution of the grain sizes. Which is known as normal grain growth [39, 40] with a grain size in the 22 - 116 nm range, for which the average is 69 nm that corresponds approximately to the film thickness. By incorporating Ammonium Acetate into the deposition bath, the deposited CdS film revealed grain growth, where the largest grains are those of 166 nm in size. However the film maintained the small grains of 22 nm at the film/substrate region (film matrix). Additionally, the films reveal an average grain size of 100 nm that is still approximately

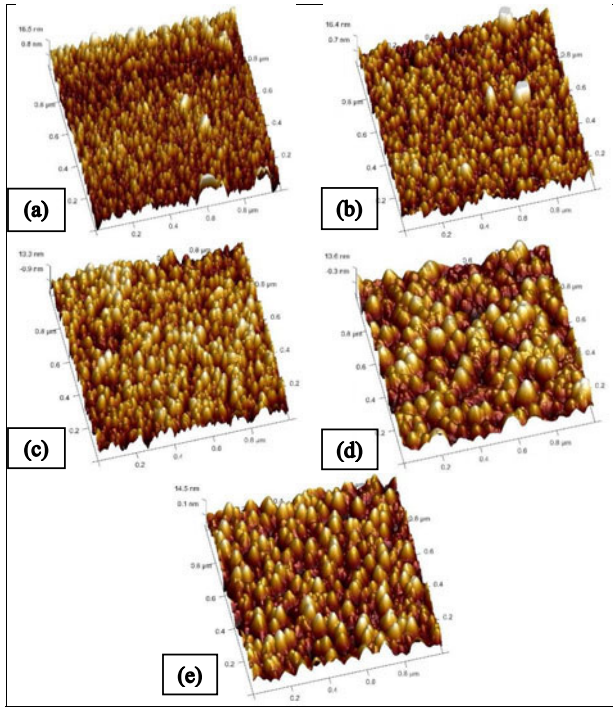

Figure 5. AFM 3D images for CBD-CdS films with corresponding ammonium acetate concentrations of (a) 0 mM , (b) 3 mM, (c) 6.7 mM, (d) 10.4 mM, and (e) 12.2 mM.

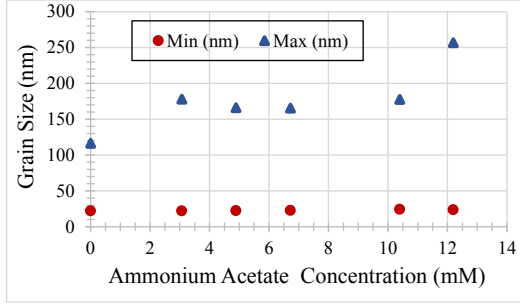

Figure 6. Grain diameter for CdS thin films as a function of the Ammonium Acetate concentration in the deposition bath.

corresponds to the film thickness; where the grain size growth is linearly proportional to the thickness of the film. The film structure exhibits network or chains of grains with adjacent grain boundaries that intersect at the surface of the film. Which might be correlated to the stagnation of normal grain growth that the film structure reached at low and intermediate level of Ammonium Acetate concentrations of the deposition bath, from 3.07 mM to 6.72 mM [41]. This is indicated by the non-significant increase and/or slight reduction in the grain size with increasing the Ammonium Acetate concentrations and its corresponding film thickness, when comparing figure 6 and figure 2. Consequently a nonlinear relation is revealed between the CdS film's grain growth and its thickness with increasing the Ammonium Acetate concentrations up to 6.72 mM in the deposition bath. On the other hand, at higher level of Ammonium Acetate concentrations of 10.4 mM and 12.2 mM, the CBD-CdS films exhibit a secondary (also known as abnormal) grain growth, as such the grains on the film surface reach average of 178 nm and 257 nm in size, respectively [39, 40, 42]. The slight increase in the growth of surface grains results in developing a bimodal grain size distribution. Which might be formed due to reduction in the total energy of the matrix and the total energy associated with normal grain boundaries. Grain coalescence is evidence forming clusters of larger grains; additionally the grain domes and its grain boundaries feature finer grains. It is believed that these features are caused by the homogeneous nucleation of CdS particles within the growth bath and their subsequent deposition on the film surface. The homogeneous nucleation leads to impurity segregation in a form of precipitates of the Cd-complexes species which mainly can occur at the grain boundaries and/or grain surfaces [43, 44]. The film structure modification is occurred by means of its transformation from monomodal to bimodal growth distribution where a secondary layer of large grains is formed at the top surface of the film, leaving behind an underneath layer of small grains. This transformation might be due to the chemical reaction change in the bath where both heterogeneous reaction is competing with homogenous reaction. It appears that the homogeneous reaction has a significant effect and a major contribution to the film growth and its structure at high concentrations of Ammonium Acetate of the deposition bath.

The measured RMS surface roughness for all CdS films is shown in Figure 7. Accordingly, the RMS roughness is decreasing from 4.37 nm to 4.16 nm with incorporating Ammonium Acetate into the deposition bath up to 10.4 mM. Then the RMS roughness changes its behavior and increases to reach 4.34 nm with further increasing of the Ammonium Acetate concentrations up to 12.2 mM. It appears that the decrease in the CBD-CdS film surface roughness with incorporating the Ammonium Acetate into the deposition bath is related to the grain growth and its coalescence. However for the increase in grain growth and significant contribution of the homogeneous nucleation to the film growth mechanism results in increasing the film surface roughness at high Ammonium Acetate concentration level.

Using the $\theta/2\theta$ XRD technique, X-ray patterns were obtained for all CBD-CdS films grown at different Ammonium Acetate concentration from 0 to 12.2 mM. As illustrated in figure 8, the $\theta/2\theta$ XRD patterns revealed that all CdS films exhibit a hexagonal (wurtzite) structure with a tendency toward strong <002> texture with increasing the concentration of Ammonium Acetate in the deposition bath, where the (002) plane has the lowest surface energy.

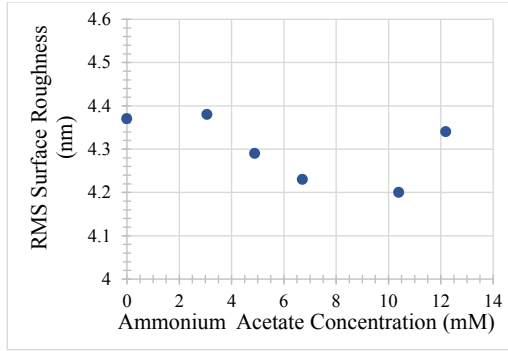

Figure 7. RMS AFM surface roughness for CBD-CdS films as a function of Ammonium Acetate concentration of the deposition bath.

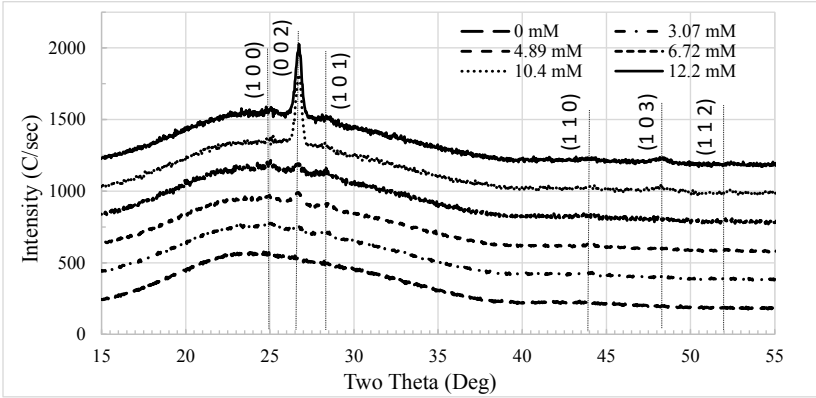

Figure 8. XRD patterns for CBD-CdS films. The dotted lines for randomly oriented powder CdS sample are shown with the highest three Bragg peaks in addition to three weaker Bragg peaks (JCPDS 01-074-9665).

(100), (002), (101), and (110) diffraction lines were analyzed by the computer program PeakFit [45]. The program modeled XRD diffraction lines by fitting them with a Pearson VII curve. The relative intensity of the (101) diffraction line to the (002) diffraction line was examined as a function of the CBD-CdS films associated Ammonium Acetate concentration. Figure 9 shows that this ratio is highest at the low Ammonium Acetate concentration (but less than the random powder value of 2.18) and it decreases toward a relative intensity near 0.1 at the highest concentration. Thus, there is a trend from a weaker (002) texture toward a stronger (002) texture as the concentration of Ammonium Acetate increases in the deposition bath. This

indicates that the films have a strong c-axis orientation aligned perpendicular to the substrate, which corresponds to those grains with low surface energies [41]. Furthermore, the peak centers for each diffraction line for all CdS films, which were calculated from the fit, were used to calculate the lattice parameter by applying Cohen's least-squares method for the hexagonal system, as described elsewhere [46]. The computer program Mathematica [47] was used to solve the matrices required for Cohen's method. Figure 10 shows the lattice parameters for CBD-CdS films as a function of Ammonium Acetate concentrations incorporated into the deposition bath. There is a clear reduction or shrinkage in the CdS unit cell lattice parameters with increasing Ammonium Acetate concentration. However, at the maximum applied Ammonium Acetate concentration of 12.2 mM, the CdS lattice parameters are close to the value expected from powdered CdS, where $a_o = 4.0907$ Å and $c_o = 6.6411$ Å (JCPDS card 01-074-9665). Thus, all CBD-CdS films are as

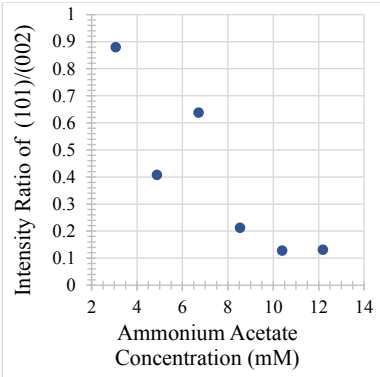

Figure 9. The relative intensity of (101) to (002) diffraction lines from CBD-CdS films.

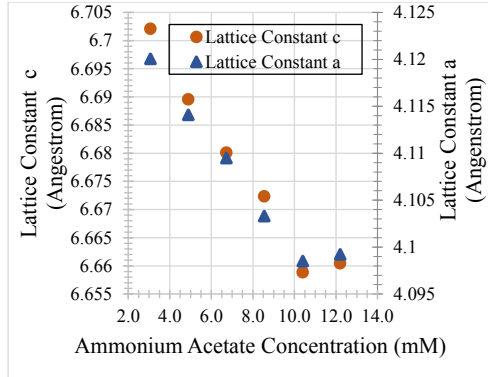

Figure 10. Lattice constants a and c, calculated using Cohen's method for the CdS thin films.

expected under a compressive stress state resulting in the lattice expansion shown in figure 10 which reaches its maximum at the lowest range of applied concentrations of Ammonium Acetate. The expansion of the unit cell might be due to the high concentration of interstitial ions that exceeds the concentration of vacancies in the films, and it occurs for the planes parallel to the film plane [48,49]. However, for the CdS films deposited with high concentrations of Ammonium Acetate, the compression stress and thus the unit cell expansion become weaker as indicated by the unit cell size shrinkage. Where according to the EDS chemical composition and for the films deposited under high range of Ammonium Acetate concentrations, the ratio of Cd to S is beyond stoichiometry. Consequently, the S vacancies have an influence over that of the Cd interstitials to decrease the unit cell size, where the radius of the S ions (172 pm) is larger than that of the Cd ions (109 pm) [50].

The CdS films showed a decrease in the transmittance (not shown here) with increasing the Ammonium Acetate concentration of the deposition bath. Which can be related to the

increase in the grown film thickness accompanied by increase in the crystalline defects such as grain boundaries and dislocations, impurities, and film stress due to lattice deformation [51-53]. All films exhibited transmittance between 70% and 90% in the visible region, and showed the fundamental absorption edge in the range 480 - 540 nm. The reflection spectra (also not shown here) of the films decreases with increasing the incorporation of Ammonium Acetate concentrations into the deposition bath. Where, the reflectance of light is affected by film surface roughness and grain size. As such the irregularity in shapes and high relative random orientation of the small grains result in additional optical scattering and absorption that is taking place at the grain boundaries. Furthermore, the optical absorption coefficients α (cm^{-1}) for the films was derived from the transmission and reflection measurements, taking into the consideration the film thickness. Then for direct band gap semiconductor as CdS, the band gap (E_{gap}) was obtained by plotting $(\alpha h\nu)^2$ over the photon energy (hν), as shown in figure 11, and extrapolating a straight line to intercept the horizontal hν axis.

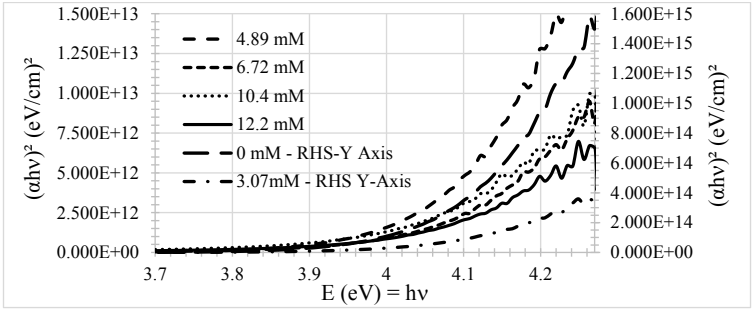

Figure 11. $(\alpha h\nu)^2$ is plotted as a function of hν used to extrapolate the energy gap value for each CBD-CdS film.

The extrapolated optical bandgap values of the CdS films are plotted in Figure 12 as a function of the associated Ammonium Acetate concentration of the deposition bath. Consequently, it can be noticed that the band gap of the CdS films increases from 3.54 eV up to 3.82 eV, a value which is associated to the highest concentrations of Ammonium Acetate applied into the growth bath. Such values of the band gap are larger than the reported value for wurtzite CdS (2.41±0.01eV) [54]. The high value of the energy gap of the CdS films is expected due to the lattice expansion causing high compression stress in the films that decreases with increasing the film thickness and its associated Ammonium Acetate concentrations of the growth bath [52, 53]. However, as the CdS film saturates in its thickness with further increasing Ammonium Acetate concentrations of the CBD; the density of defects and impurities increase in the films as a result of deviating from stoichiometry and possible formation of a secondary porous over-layer. Eventually, this results in further increasing the energy gap of the films and lattice shrinkage.

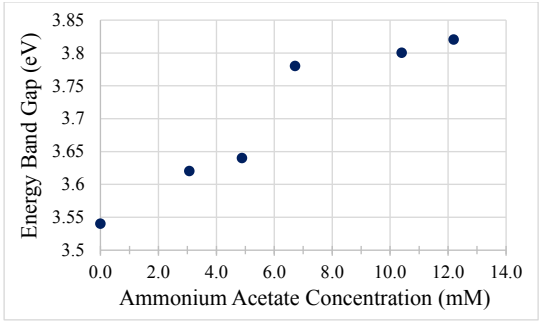

Figure 12. Energy band gap for CdS films as a function of the Ammonium Acetate concentration of the deposition bath.

SUMMARY

CdS films were grown on glass substrates by chemical bath deposition technique (CBD). By incorporating Ammonium Acetate into the chemical bath, a growth transformation from monomodal to bimodal distribution as the Ammonium Acetate concentration increases of the deposition bath was revealed by AFM imaging. The deposited films exhibited clusters of grains with domed tops and fine surface sub-grains that became less significant at high investigated level of Ammonium Acetate concentrations. These results emphasized the influence of the competing reactions in the chemical bath between heterogeneous and homogenous growth mechanisms. Where the latter is more significant at high concentrations of Ammonium Acetate, resulting in formation of a secondary porous over-layer.

The grain growth and film thickness were found linearly increasing with the concentration of Ammonium Acetate at low and intermediate level; however the grain growth and film thickness were found to saturate at high investigated Ammonium Acetate concentrations. All CdS films were under compression stress accompanied with expansion in the unit cell, however the film stress became weaker and the unit cell shrink in size with further increasing the Ammonium Acetate concentration. Which was correlated to the excess of S vacancies over Cd Interstitials in the unit cell. The films had high energy band gap within the range of 3.54 eV - 3.82 eV that was interpreted due to the deviation in film stoichiometry and possible increase in the density of defects and impurities contents in the films.

REFERENCES

1. Q.Q. Liu, J.H. Shi, Z.Q. Li, D.W. Zhang, S.M. Huang; J. Phys. **B405** (2010), 4360-4365
2. F.Liu, Y.Lai, J.Liu, B.Wang, S.Kuang, Z.Zhang, J.Li, Y.Liu, J.Alloys and Comp. **493** (2010) 305-308
3. Limei Zhou, Xiaofei Hu, Sumei Wu; Effects of Deposition Temperature on the Performance of CdS Films with Chemical Bath Deposition; J. Surface and Coating Technology **228** (2013), pp. 5171-5174

4. Vigil O, Zeleya-Angel O, and Rodriguez Y; Semicond. Sci. Technol. **15** (2000), p. 259.
5. I.Kaur, D.K. Pandya, and K.L. Chopra, J. Electrochem. Soc. **127**, 943 (1980).
6. D.Lincot and J.Vedel, Proc. 10th E.C. Photovolt. Solar Energy Conf., **931**(1991).
7. D.H. Rose, F.S. Hasoon, R.G. Dhere, D.S. Albin, R.M. Ribelin, X.S. Li, Y. Mahathongdy, T.A. Gessert and P.Sheldon; Fabrication Procedures and Process Sensitivities for CdS/CdTe Solar Cells; Progress in Photovoltaics Research and Applications; Prog. Photovolt: Res. Appl. **7** (1999) pp. 331-340.
8. D.Lincot, R. Ortega-Borges, J.Vedel; M.Ruckh, J. Kessler, K.O. Velthaus, D.-Hariskos, H.W. Schock; Chemical Bath Deposition of CdS on CuInSe2 Combining Dry and Wet Processes for high Efficiency Thin Film Solar Cells: Proceeding of 11th E.C.Photovoltaic Solar Energy Conference (1992); pp. 870-873.
9. M.Tomakin, A. Altunbas, E.Bacaksiz, S.Celik; J. Thin Solid Films **520** (2012) 2532-2536.
10. N.R. Paudel, K.A. Wieland, A.D. Compaan; J.Solar Ener. Mater. & Soalr Cells **105** (2012) 109-112.
11. J.Nishino, S. Chatani, Y. Uotani, Y.Nosaka; J. Electroana. Chem. 473 (1999) 217-222.
12. G.Brunthaler, M.Lang, A.Forstner, C.Giftge, D.Schikora, S.Ferreira, H.Sitter, K.Lischka; J.Cryst.Growth **138** (1994)559.
13. R.P. Vaudo, D.B. Eason, K.A.Bowers, K.J.Gosset, J.W. Cook, J.W. Schetsina; J.Vac. Sci. Technol. **B11** (1993) 875.
14. H.Matsumoto, A. Nakayama, S.Ikegami, Y.Hiori; Jpn. J. Appl. Phys. **15** (1980) 129.
15. H.C. Chou, A. Rohatgi, E.W. Thomas, S. Kamra, A.K. Bhat; J.Electrochem Soc. **142** (1992) 254.
16. H.C. Chou, A. Rohatgi; J. Electron. Mater. **23** (1994) 31.
17. H. S. Kwork, J.P. Zheng, S. Witanachchi, P.Mattocks, L.Shi, Q.Y. Ying, X.W. Wang, D.T. Shaw; Appl. Phys. Lett. **52** (1988) 1095.
18. T.L. Chu, J. Britt, C.Ferekides, C. Wang, C.Q. Wu; IEEE Trans. Electron. Device Lett. **13** (1992) 303.
19. S. Bonilla, E.A. Dalchiele, Thin Solid Films **204** (1991) 397.
20. M.A.Green, K.Emery, Y.Hishikawa, W.Warta, and E.D. Dunlop, Solar Cell Efficiency Tables (version 46); Prog. Photovolt: Res. Appl.**23** (2015) pp.805 - 812.
21. A.E. Baumann, K.Hynes, and J.Herrero, Proc. 2nd World Conf. Photovolt. Solar Energy Conv., 735 (1998).
22. M.A. Barote, A.A. Yadav, E.U. Masumdar; J.Phys. **B 406** (2011) 1865-1871.
23. S.Prabahar, M.Dhanam; J. Crys. Growth **285** (2005) 41-48.
24. T.L. Chu, S.S. Chu, C.Q. Wu, J. Britt, And C. Wang, in Proceedings of the 22nd IEEE Photovoltaic Specialists Conferences, (1991) 952.
25. Raul Ortega-Borges and Daniel Lincot; "Mechanism of Chemical Bath Deposition of Cadmium Sulfide Thin Films in the Ammonia-Thiourea System inSitue Kinetic Study and Modelization; J.Electrochem. Soc. **Vol. 140**, NO. 12 (1993) pp.3464-3473.
26. D. Lincot and R. Ortega-Borges, ibid, **139** (1992) 1880.
27. J.Y. Choi, K-J Kim, JI-B Yoo, and D. Kim; Properties of Cadmium Sulfide Thin Films Deposited by Chemical Bath Deposition with Utrasonication; Solar Energy **Vol. 64** Nos 1-3, (1998) pp.41-47.
28. Limei Zhou, Xiaofei Hu, Sumei Wu; Effects of PH Value on Performance of CdS Films with Chemical Bath Deposition, Advanced Materials Research **Vols. 557-559** (2012) pp.1941-1944.

29. A.Kariper, E. Guneri, F. Gode, and C. Gumus; Effect of PH on the Physical Properties of CdS Thin Films Deposited by CBD; Chalcogenide letters, **Vol. 9, NO. 1** (2012). Pp. 27-40.
30. R.Y. Munikrishna, V.P.M Nagendra, IOSR J.Appl. Phys. **4** (2013) 3464.
31. S. Mahanty, D. Basak, F. Rueda, and M. Leon; J. Electron Mater.**28** (1999) 559.
32. B.R. Lanning, J.H. Armstrong; Int. J. Sol. Energy **12** (1992) 247.
33. I.O. Oladeji, L. Chow, J.R. Liu, W.K. Chu, A.N.P. Bustamante, C. Fredricksen, A.F.Schulte; Thin Solid Films **359** (2000) 154-159.
34. I.O. Oladeji and L. Chow; Optimization of Chemical Bath Deposited Cadmium Sulfide Thin Films; J. Electrochem. Soc. **Vol. 144**, NO. 7 (1997).
35. T.L.Chu, Shirley S. Chu, N. Schultz, C. Wang, and C.Q. Wu; "Solution Grown Cadmium Sulfide Films for Photovoltaic Devices", J. Electrochem. Soc. **Vol. 139**, NO.9, (1992), pp. 2443-2446.
36. A.Kylner, A. Rockett, and L.Stolt, "Oxygen in Solution Grown CdS Films for Thin Film Solar Cells, Solid State Phenomena **Vols. 51-52** (1996) pp. 533-540.
37. A.Kylner and Mikael Wirde; "A High Resolution X-Ray Photoelectron Spectroscopy Study of Carbon-Nitrogen Impurity in Chemical Bath Deposited CdS Thin Films"; Jpn. J. Appl. Phys. **Vol.36** (1997) pp.2167-2175.
38. A.Kylner, and E.Niemi, "Chemical Bath Deposited CdS films with Different impurity Concentrations – Film Characterization and Cu(In,Ga)Se_2 Solar Cell Results"14th European photovoltaic Solar Energy Conference, Parcelona, Spain (1997) pp.1326-1329.
39. E.S. Machlin, Materials Science in Microelectronics: The Relationships between Thin Film Processing and Structure (Giro Press, N.Y., 1995).
40. C.V. Thompson, J. Appl. Phys. **58**, 763 (1985).
41. C.V. Thompson, Annu. Ref. Mater. Sci. **20**, 245 (1990).
42. C.C. Wong, H.I. Smith, and C.V. Thompson, Appl. Phys. Lett. **48**, 335 (1986).
43. F.S. Hasoon, M.M. Al-Jassim, A.Swartzlander, P.Sheldon, A.A. Al-Douri, and A.A. Alnajjar, "The morphology of CdS Thin Films Deposited on SnO2-Coated Glass Substrates", 26th IEEE PVSC, Anaheim, California (1997). NREL Report NO.CP-530-23580.
44. J.D. Webb, D.H.Rose, D.W. Niles, A. Swartzlander, and M.M. Al-Jassim, Proceedings 26th IEEE PVSC. (1997). P. 399.
45. PeakFit V4.11: Peak Separation and Analysis Software, Manufactured by SYSTAT Software Inc. For more information visit WWW. Site at http://www.systatsoftware.com; accessed on March 25th, 2016.
46. B.D. Cullity and S.R. Stock, Elements of X-Ray Diffraction, 3rd ed. (Prentice Hall, NY, 2001).
47. Mathematica V4.2 software, Manufactured by Wolfram Research Inc. For more information visit www. Site at http://www.wolfram.com; accessed on March 25th, 2016.
48. H.Kaneko, M.Hasunuma, A.Sawabe, T.Kawanoue, Y.Kohanawa, S. Komatsu, and M.Miyauchi, Proc. IEEE/IRPS, 194 (1990).
49. X. L. Liu, Y.J. Zhu, V. Valdna, Mater. Lett. **63** (2009) 1085.
50. R.D. Shannon, "Revised Effective Ionic Radii and Systematic Studies of Interatomic Distances in Halides and Chalcogenides". Acta Cryst **A32** (1976) pp. 751-767.
51. M.M. Al-Jassim, R.G. Dhere, K.M. Jones, F.S. Hasoon, P.Sheldon, "The Morphology, Microstructure, and Luminescent Properties of CdS/CdTe Films", Proceeding of 2nd World

Conference and Exhibition on Photovoltaic Solar Energy Conversion, Vienna, Austria (1998).
52. S.Jimenez-Sandoval, M.Melendez-Lira, and I.Hernandez-Calderon, "Crystal Structure and Energy Gap of CdTe Thin Films Grown by Radio Frequency Sputtering", J.Appl. Phys. **72 (9)**, (1992), pp.4197-4202.
53. M.E. Ozsan, D.R. Johnson, M.Sadeghi, D.Sivapathasundaram, G.Goodlet, M.J.Furlong, L.M.Peter, A.A. Shingleton, "Optical and Electrical Characterization of CdS Thin Films", Journal of Materials Science: Materials in Electronics **7**(1996) pp.119-125
54. L.I.Berger, Semiconductor Materials (CRC Press, Florida, 1997).